Stem Cell Reports
Article

OPEN ACCESS

XIST Derepression in Active X Chromosome Hinders Pig Somatic Cell Nuclear Transfer

Degong Ruan,[1,2,3,6] Jiangyun Peng,[1,2,3,6] Xiaoshan Wang,[1,2,3,6] Zhen Ouyang,[1,3,6] Qingjian Zou,[1,3] Yi Yang,[1,3] Fangbing Chen,[1,2,3] Weikai Ge,[1,2,3] Han Wu,[1,2,3] Zhaoming Liu,[1,3] Yu Zhao,[1,3] Bentian Zhao,[1,3] Quanjun Zhang,[1,3] Chengdan Lai,[1,3] Nana Fan,[1,3] Zhiwei Zhou,[1,2,3] Qishuai Liu,[1,2,3] Nan Li,[1,2,3] Qin Jin,[1,2,3] Hui Shi,[1,2,3] Jingke Xie,[1,2,3] Hong Song,[1,3] Xiaoyu Yang,[1,5] Jiekai Chen,[1,3] Kepin Wang,[1,3,*] Xiaoping Li,[1,3,*] and Liangxue Lai[1,3,4,*]

[1]CAS Key Laboratory of Regenerative Biology, Joint School of Life Sciences, Guangzhou Institutes of Biomedicine and Health, Chinese Academy of Sciences, Guangzhou Medical University, Guangzhou 510530, China
[2]University of Chinese Academy of Sciences, Beijing 100049, China
[3]Guangdong Provincial Key Laboratory of Stem Cell and Regenerative Medicine, South China Institute for Stem Cell Biology and Regenerative Medicine, Guangzhou Institutes of Biomedicine and Health, Chinese Academy of Sciences, Guangzhou 510530, China
[4]Jilin Provincial Key Laboratory of Animal Embryo Engineering, Institute of Zoonosis, College of Veterinary Medicine, Jilin University, Changchun 130062, China
[5]Institute of Physical Science and Information Technology, Anhui University, Hefei, Anhui 230601, China
[6]Co-first author
*Correspondence: wang_kepin@gibh.ac.cn (K.W.), li_xiaoping@gibh.ac.cn (X.L.), lai_liangxue@gibh.ac.cn (L.L.)
https://doi.org/10.1016/j.stemcr.2017.12.015

SUMMARY

Pig cloning by somatic cell nuclear transfer (SCNT) remains extremely inefficient, and many cloned embryos undergo abnormal development. Here, by profiling transcriptome expression, we observed dysregulated chromosome-wide gene expression in every chromosome and identified a considerable number of genes that are aberrantly expressed in the abnormal cloned embryos. In particular, *XIST*, a long non-coding RNA gene, showed high ectopic expression in abnormal embryos. We also proved that nullification of the *XIST* gene in donor cells can normalize aberrant gene expression in cloned embryos and enhance long-term development capacity of the embryos. Furthermore, the increased quality of *XIST*-deficient embryos was associated with the global H3K9me3 reduction. Injection of H3K9me demethylase *Kdm4A* into NT embryos could improve the development of pre-implantation stage embryos. However, *Kdm4A* addition also induced *XIST* derepression in the active X chromosome and thus was not able to enhance the *in vivo* long-term developmental capacity of porcine NT embryos.

INTRODUCTION

Cloned pigs have been produced by somatic cell nuclear transfer (SCNT) for many years (Lai et al., 2002; Park et al., 2001). However, the overall cloning efficiency in terms of blastocyst development and the birth of full-term pigs remains extremely low (<0.5%) (Mao et al., 2012; Yuan et al., 2014; Zeng et al., 2016). This low efficiency seriously hinders the application of genetically modified cloned pigs.

In pig cloning, many surrogates can progress to early pregnancy, but only a few pregnancies develop to term. Most implanted SCNT embryos suffer growth retardation and are eventually absorbed by surrogate sows during pregnancy (Huang et al., 2013). Comparison of the transcriptional differences among normal nuclear transfer (NT) fetuses, abnormal NT fetuses and fertilized ones would help provide insights into this phenomenon.

SCNT is a process of reprogramming differentiated cells into totipotent stem cells by oocytes (Meissner and Jaenisch, 2006; Ogura et al., 2013). The abnormal development of SCNT-derived embryos might be attributed to the aberrant reprogramming of the donor genome (Rodriguez-Osorio et al., 2012; Yuan et al., 2014). One SCNT-specific error identified in mouse is the large-scale downregulation of X chromosome-linked genes in the cloned embryos; this downregulation is mainly caused by the ectopic expression of *XIST* gene, a non-coding RNA and maternally expressed imprinted gene responsible for the X chromosome inactivation (XCI) at the pre-implantation stages of mouse development (Bao et al., 2005; Inoue et al., 2010; Matoba et al., 2011). By contrast, deletion of *XIST* or repression of *XIST* expression by specific short interfering RNA (siRNA) from the active X chromosome in the donor genome can elevate about 10-fold normal birth rate of mouse cloning (Inoue et al., 2010; Matoba et al., 2011).

In mouse, many cloned embryos also arrest before implantation stage (Liu et al., 2016). The residual status of repressive histone modifications on specific regions is a reprogramming error in these early-stage embryos (Inoue et al., 2010). The transformation of differentiated donor nuclei to a totipotent state in reconstructed embryos must overcome epigenetic barriers, such as the reduction of H3 lysine 9 methylation (H3K9me), which is the primary epigenetic determinant for the intermediate insufficient pluripotent stem cell state. The removal of such epigenetic

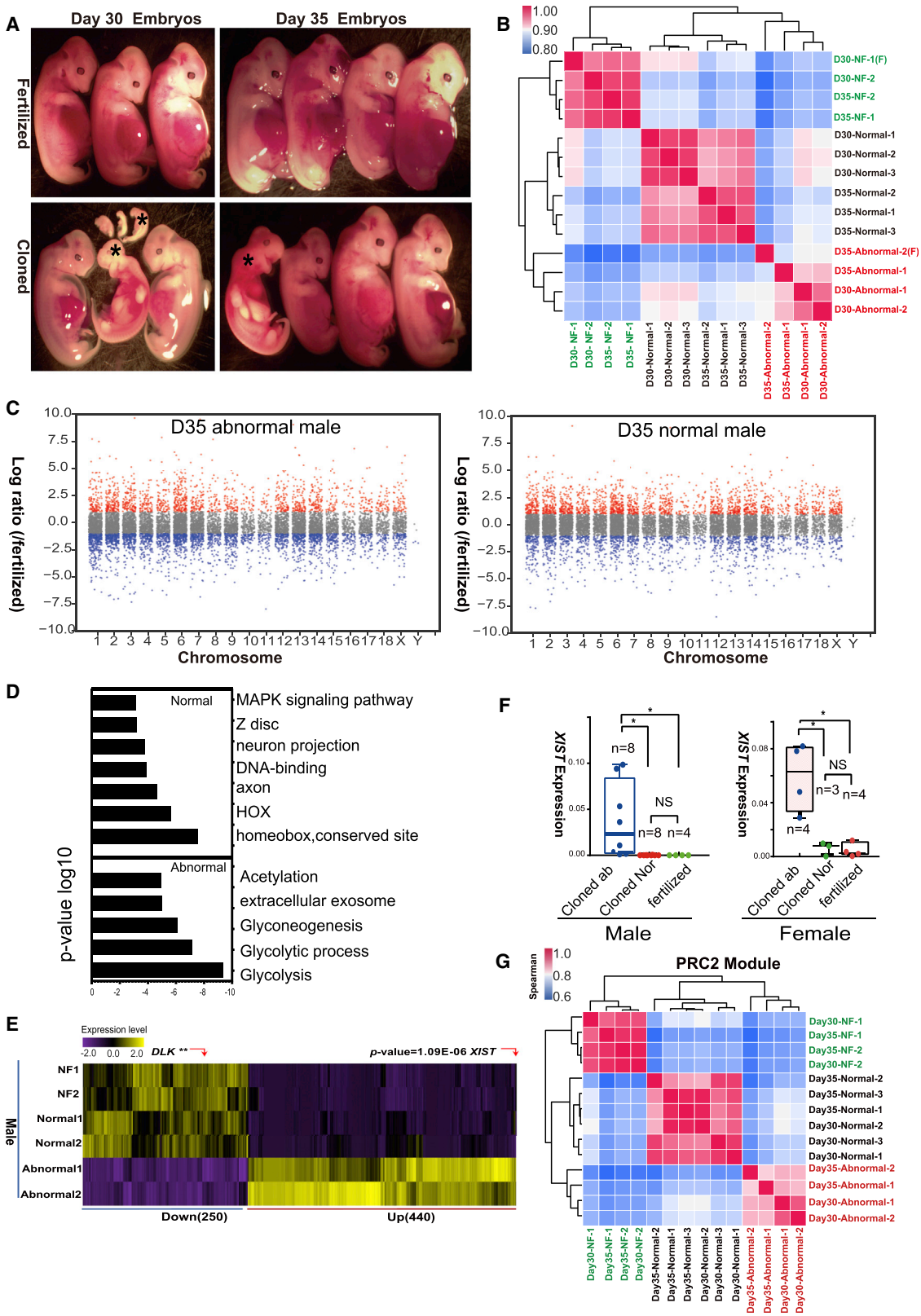

(legend on next page)

barriers produces fully reprogrammed pluripotent stem cells (Chen et al., 2013; Chung et al., 2015; Liu et al., 2016; Matoba et al., 2014). In cloned mouse embryos, gene expression abnormalities begin at the two-cell stage, which corresponds to the major wave of zygotic genome activation (ZGA) in normal embryogenesis of the mouse (Matoba et al., 2014; Schultz, 2002). Abnormal gene reactivation in cloned mouse embryos can be partly rescued through H3K9me3 demethylation using histone H3 lysine 9 trimethylation demethylases, including Kdm4b (Liu et al., 2016) or Kdm4d (Matoba et al., 2014).

In the present study, through analysis of the global transcriptome of cloned embryos we found that pig SCNT-specific abnormalities are associated with aberrant *XIST* expression and persistent H3K9me3 residues. Nullification of the *XIST* gene could significantly impede *XIST* expression, which leads to the significant reduction of global H3K9me3 level and improvement of the developmental capacity of NT embryos. We also found that injecting porcine H3K9me3 demethylase *Kdm4A* could greatly reduce the global H3K9me3 level. However, the injection of *Kdm4A* into SCNT embryos induced H3K9me3-enriched *XIST* derepression and resulted in wide-scale gene downregulation, and thus failed to improve the developmental capacity of the reconstructed pig NT embryos.

RESULTS

Global Gene Expression Pattern of Cloned Fetuses

A total of 944 NT embryos were transferred into 6 surrogates. Four of these surrogates were found to be pregnant, as confirmed by ultrasound check 25 days after embryo transfer. The fetuses with gestational periods of 30 and 35 days were collected (Table S1). Many of the fetuses underwent developmental retardation (abnormal), only a few developed normally (Figures 1A and S1A).

To define the transcriptional differences between the normal and abnormal NT embryos, tissues derived from day 30 (n = 5) and day 35 fetuses (n = 5) from the same surrogate sows were used for RNA sequencing (RNA-seq) analysis. The tissue from the *in vivo* fertilized fetuses at the same day (day 30, n = 2; day 35, n = 2) were used as the controls. The collected fetuses were sex defined and their RNA integrity was validated by agarose gel electrophoresis (Figure S1B). Comparative RNA-seq analysis revealed that the naturally fertilized, normal cloned and abnormal cloned fetuses featured different global transcriptome patterns (Figures 1B and S1C). Compared with the fertilized fetuses, the normal cloned and abnormal cloned fetuses harbored different numbers of up- and downregulated genes (Figure S1D). These genes were distributed across all the 19 chromosomes (Figures 1C and S1E). The number of commonly downregulated genes (CDGs) solely found in day 30 and day 35 normal and abnormal male cloned fetuses were 120 and 805, respectively. For the upregulated genes, a subset of 475 commonly upregulated genes (CUGs) in the normal fetuses failed to be activated in the abnormal cloned fetuses. By contrast, a subset of 267 genes was found commonly to be activated in the abnormal cloned fetuses (Figure S1F). Chromosome distribution analysis revealed that these CDGs and CUGs in both day 30 and day 35 normal and abnormal male fetuses were located not only in X chromosome but also in the other autosomes (Figure S1G). Gene ontology (GO) analysis revealed that in the abnormal fetuses (in both day 30 and day 35 fetuses), these genes (475 CUGs) that failed to be activated were enriched in embryo development pathways, while the upregulated genes (267 CUGs) appeared to be involved in metabolism (Figure 1D).

To determine the master genes correlating with fetus abortion, we further analyzed all of the up- and downregulated genes ($p < 0.05$, fold change > 2) based on the transcriptomes in all the cloned and fertilized male fetuses on

Figure 1. Global Gene Expression of SCNT Embryos

(A) Representative pig fertilized and cloned fetuses on day 30 and day 35. The fertilized and normal cloned fetuses are larger with a well-defined shape. By contrast, the abnormal fetuses are smaller and underwent growth retardation with blurry shape. Asterisks indicate the type of abnormal fetuses chosen for RNA-seq.

(B) RNA-seq analysis (Spearman correlation coefficient) of the naturally fertilized, normal cloned, and abnormal cloned pig fetuses on day 30 and day 35. D30-NF-1 and D35-abnormal-2 fetuses are female, the other fetuses are male.

(C) Relative gene expression levels of day 35 normal male cloned fetus, abnormal male cloned fetus, and fertilized male fetus are plotted on the genomic positions from all chromosomes. The genes up- and downregulated in the cloned fetuses (fold change [FC] > 2) with respect to those in the fertilized fetus are marked in red and blue, respectively.

(D) Gene ontology (GO) analysis of the commonly upregulated genes in day 30 and day 35 cloned fetuses.

(E) The differentially upregulated (440 genes) and downregulated genes (250 genes) ($p < 0.05$) of male abnormal fetuses. *XIST* is among the top 10 highest expressed genes and *DLK1* is significantly downregulated in the male abnormal fetuses. $^{**}p < 0.01$.

(F) Relative expression levels of *Xist* were quantified in individual fetuses. *XIST* is an X-linked gene and was separately quantified in independent female and male fetuses. Error bars indicate ± SEM. $^{*}p < 0.05$, two-tailed unpaired Student's t test.

(G) Spearman correlation coefficient analysis of PRC2 module between the groups of day 30 and day 35 fetuses.

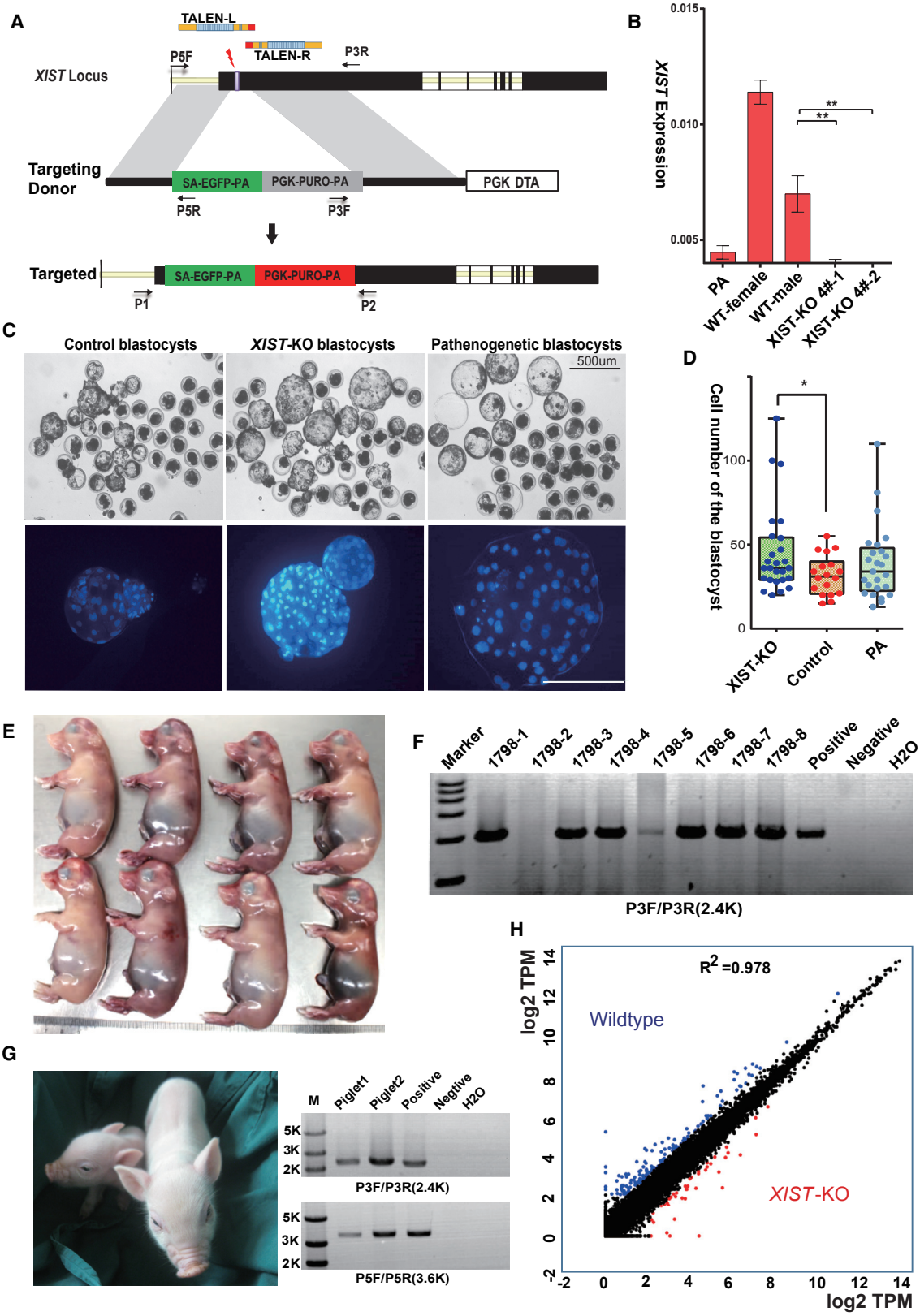

(legend on next page)

day 30 and day 35. We found one non-coding RNA *XIST*, which is required for full-term normal growth and plays important roles in X chromosome-wide gene inactivation in mouse, was expressed at a significantly higher level (among the top 10) in the abnormal cloned fetuses than in the normal and fertilized counterpart (Figure 1E; Table S2). qRT-PCR analysis further confirmed that upregulation of *XIST* expression only existed in abnormal fetuses (both male and female cloned fetuses) (Figure 1F). Imprinted genes *DLK1* and *IGF2* also differentially expressed between the groups in day 30 and day 35 fetuses (Figure S1H).

Previous studies demonstrated that *XIST* is the master regulator of XCI and provokes the stable silencing of the entire X chromosome. *XIST* would recruit polycomb repressive complex 2 (PRC2) by unknown mechanism and showed linear correlations of PRC2-mediated tri-methylation of lysine 27 of histone H3 (H3K27me3) (Brockdorff, 2017; Cerase et al., 2015; da Rocha and Heard, 2017). We next assessed the whole genome repressive pattern (PRC2 module) by performing principal-component analysis (PCA) and gene set enrichment analysis of microarray data for the expression of polycomb complex target genes. These analyses revealed that, in comparison with fertilized fetuses, the day 30 normal cloned fetuses had already attained high-fidelity transcription of the repressive patterns that were indistinguishable from the day 35 ones but were significantly different from the abnormal cloned fetuses (Figures 1G and S1I). The day 30 and day 35 abnormal cloned fetuses harbored a subset of up- and downregulated genes, which were down- and upregulated in the normal cloned and fertilized fetuses, respectively (Figure S1J). Collectively, the bioinformatics studies revealed that highly ectopic expression of *XIST* was closely linked to fetus abortion and would greatly hinder pig somatic NT.

Development Capacity of Reconstructed Embryos Derived from *XIST*-Null Donor Cells

The results above showed that the high ectopic expression of the *XIST* gene may cause developmental retardation in the cloned fetuses. To determine whether the impeded *XIST* expression in donor cells could improve the developmental capacity of the cloned fetuses, we nullified the *XIST* gene of both male and female porcine fetal fibroblasts using the TALEN gene-editing system before using them as donor cells. A pair of TALENs targeting the functional repeated region in the first exon of the pig *XIST* gene (Figures 2A and S2A) was designed. To disrupt *XIST* expression, an EGFP CDS and puromycin-resistance cassette were inserted downstream the *XIST* promoter (Figure 2A). In the process, EGFP was used as an indicator of *XIST* expression nullification in the reconstructed embryos. The correct targeted mutation of selected fibroblast colonies was confirmed by PCR and sequencing with two pairs of primers, which resulted in products with the length of 2,379 and 3,727 bp, respectively (Figures S2B and S2C). Fifteen cell lines (male and female) with correct mutations were achieved (Table S3). The wild-type allele of mutant female clones was untouched, which was confirmed by sequencing (Figure S2D). The NT embryos derived from the mutant cells emitted green fluorescence. This result further validated the vector and the correct mutation in the donor cells (Figure S2E). Day 6 blastocysts generated from male *XIST*-deficient cells (n = 2 male clones) also showed barely detectable *Xist* expression, which was significantly lower than the wild-type male blastocysts (Figure 2B). When the mutant cells (male and female) were used as donors for SCNT, the rate of blastocysts derived from *XIST*-deficient cells (121/332, 36.4%) was significantly higher than that of blastocysts derived from the control cells (101/398, 25.4%) ($p < 0.01$,

Figure 2. *XIST* Mutant Fibroblast Cells and Their Developmental Capacity

(A) Schematic of the genomic region containing the pig *XIST* gene and the targeting homologous recombination vector used for electroporation. In the mutant locus, the genomic sequence was replaced with an EGFP and puromycin expression cassette. Exons are represented as black boxes.

(B) Relative expression of *Xist* in day 6 *in vitro* blastocysts (mean ± SD, two-tailed unpaired Student's t test, n = 3 biological replicates from 3 separate embryo extracts **$p < 0.01$).

(C) Day 6 blastocyst phenotype from *XIST*-nullified and wild-type fibroblast cells. Parthenogenetic blastocysts served as control to demonstrate oocyst quality. Scale bar, 500 μm. Representative DAPI staining image of day 6 *in vitro* embryos from the *XIST*-nullified donor cell, wild-type cell, and parthenogenetic blastocyst. Scale bar, 500 μm.

(D) Statistical analysis of the total cell number per blastocyst from the *XIST*-null (n = 26) and wild-type fibroblasts (n = 18), with parthenogenetic blastocysts (n = 25) as the control. Mean ± SEM, two-tailed unpaired Student's t test, n = 3 biological replicates to collect embryos. *$p < 0.05$.

(E and F) One of the surrogate sows, 1,798, which was transplanted with 100 male *XIST*-defective and 100 male wild-type reconstructed embryos, underwent caesarean section on day 40 of gestation. Seven normal fetuses showed *XIST*-defective mutation, whereas one normal fetus was wild-type. Primer sequences are listed in Table S5. PCR products are 2,379 bp.

(G) One of the surrogate sows, which was transplanted with 246 wild-type and 127 *XIST*-KO reconstructed NT embryos, gave birth to two piglets. PCR identification showed these piglets generated from *XIST*-defective embryos.

(H) Scatterplots comparing gene expression levels between *XIST*-KO and wild-type fetuses. Genes that expressed higher in *XIST*-KO (FC > 2.0, XIST-KO high) and higher in wild-type fetus (FC > 2.0, wild-type high) are colored red and blue, respectively.

n = 6 replicates) (Table S3). *XIST*-deficient cells also could result in reconstructed embryos with enhanced quality, as the size of most blastocysts was increased, and many of them hatched out of the zona pellucida (n = 3 replicates) (Figures 2C and S2F). Furthermore, the average cell number of *XIST*-deficient embryos (N = 26, mean = 45) was significantly higher than that of the control group embryos (N = 18, mean = 34), and even higher than that of the parthenogenetic (PA) embryos (N = 25, mean = 39), which served as an index of oocyte quality (Figures 2C and 2D).

To determine whether the cells containing a *XIST*-deficient Xa (male fibroblasts) hold long-term growth advantages over the control cells, a total of 530 embryos derived from male *XIST*-deficient embryos and 953 embryos derived from wild-type cells were transferred into the same 5 surrogates. All 5 surrogates were found pregnant confirmed by ultrasound confirmation 25 days after embryo transfer (Table S3). One of the surrogates transferred 100 male *XIST*-deficient embryos and 100 wild-type male embryos was killed 40 days after embryo transfer (Figure 2E). Eight male fetuses of normal sizes were retrieved. Genotyping results identified by PCR showed seven out of the 8 fetuses harboring the *XIST* mutation (Figure 2F). Two of the 4 other surrogates, which were transferred 193 male *XIST*-deficient embryos and 404 wild-type embryos in total, developed to full-term pregnancies. Six living piglets (male) were also delivered. Four of the piglets were *XIST*-knockout (*XIST*-KO) piglets, and two were wild-type piglets, as confirmed by PCR and sequencing (Figure 2G). Combing with the fetuses retrieved from the killed recipient, we obtained a cloning efficiency 6.9 times higher when *XIST*-deficient cells were used as donor nuclei (11/530, 2.07%) than when wild-type cells (3/953, 0.3%) were employed (Table S3). This result indicates that the reconstructed embryos from the *XIST*-null cells held a higher developmental competency.

qRT-PCR showed that all the eight fetuses did not express *XIST* (Figure S2G). RNA-seq analysis revealed that the *XIST*-null fetuses and normal wild-type fetuses shared highly similar transcriptomes ($R^2 = 0.978$; Figure 2H). The expression levels of the imprinted genes, including *DLK1, H19*, and *IGF2*, showed no remarkable difference between the *XIST*-KO fetuses and the normal wild-type ones (Figures S2H and S2I).

Gene Expression Related to Pluripotency and Epigenetics Status in Reconstructed Embryos Derived from *XIST*-Null Donor Cells

To further evaluate the quality of the blastocysts generated from *XIST*-deficient cells, we performed DNA methylation analysis and compared gene expression profile to delineate the reprogramming degree differences between the groups.

The DNA demethylation of some transcription factors and imprinted genes can reflect the degree of reprogramming completion (Huan et al., 2015; Mao et al., 2015; Zhao et al., 2013). Therefore, we analyzed the DNA methylation statuses of *POU5F1*, *XIST*, and *IGF2* loci in the porcine female donor cells and a variety of day 6 *in vitro* culture embryos including NT, PA, and *in-vitro*-fertilized (IVF) (mix of male and female) embryos. The *POU5F1* locus methylation level was relatively higher in the differentiated donor cells (30/140, 21.4%) than in the embryos. The *POU5F1* locus DNA methylation level greatly decreased in the embryos derived from *XIST*-deficient cells (1/140 = 0.7%) compared with parthenogenetic embryos (PEs) (13/140 = 9.3%) and wild-type cell-derived embryos (10/140 = 7.1%). However, the former level was very close to that in the IVF embryos (0%). In the female donor cells, the DNA methylation level in the *XIST* loci showed completely unmethylated and completely methylated status in the inactive and active allele, respectively. In day 6 *in vitro* culture embryos, the IVF (mix) and PA embryos had only unmethylated alleles, while control embryos had mostly unmethylated but still had three to four amplicons with elevated methylation, while *XIST*-KO embryos showed only one significantly methylated amplicon. The *IGF2* loci of the donor cells were highly methylated (122/170 = 71.7%). In the PA embryos, the *IGF2* loci were also highly methylated (54.7%). The NT embryos exhibited a much lower methylation level than those in the donor cells and PEs. The methylation level of *XIST*-null cell-derived embryos (48/170 = 28.2%) was also moderately reduced relative to that of the wild-type cell-derived embryos (57/170 = 33.5%), and very close to that of the IVF embryos (48/170 = 28.2%) (Figure 3A).

To explore the potential mechanism of the nullification of *XIST* gene in improving the development of cloned embryos, the transcriptional differences between early *XIST* nullification embryos and control embryos in *in vitro* culture for 6 days were compared by RNA-seq analysis. Comparative RNA-seq analysis revealed that the IVF (n = 2), wild-type cell-derived (n = 2), and *XIST*-deficient cell-derived embryos (n = 2) also featured different global transcriptome patterns but *XIST*-deficient cell-derived embryos were closer to IVF embryos (Figures 3B and S3A). Compared with IVF embryos, the wild-type cell-derived embryos had 2,136 commonly differentially dysregulated genes, of which 1,286 were upregulated (CUGs) and 850 were downregulated (CDGs) (Figure S3C). These dysregulated genes were distributed across all the 19 chromosomes (Figure S3D). Comparing with the wild-type cell-derived embryos, *XIST*-deficient cell-derived embryos had fewer upregulated genes (536 versus 1,255) and downregulated genes (562 versus 1,497) (Figure S3E). And these genes were also distributed across all 19 chromosomes

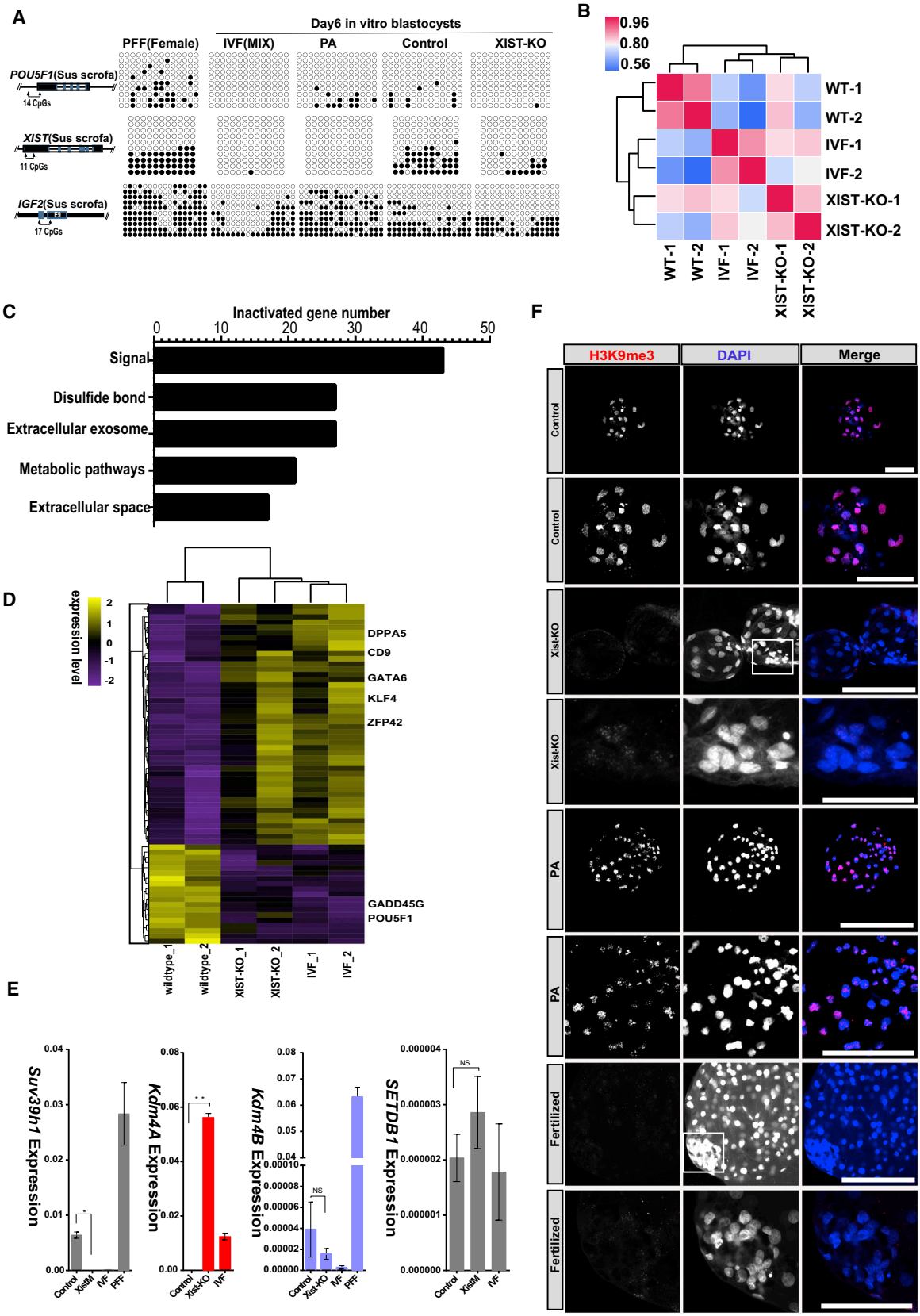

(legend on next page)

(Figure S3F). We specially examined the inactivated genes (54 genes, mean = 0) in the wild-type cell-derived embryos. The result showed these inactivated genes were mainly enriched in signal pathways (Figure 3C).

Reprogramming completion degree is directly associated with developmental capacity of NT embryos. We then examined the pluripotency network (ESC module) between the IVF, *XIST*-deficient, and wild-type cell-derived embryos. A total of 386 embryonic stem cell related genes were analyzed, including transcription factors for maintaining pluripotency and pluripotency repressors. *XIST*-KO embryos featured a pluripotency network similar to IVF embryos. The expression level of inner cell mass (ICM) genes, such as *GATA6*, *ZFP42*, *KLF4*, *DPPA5*, and *CD9*, were higher in the *XIST*-deficient embryos than in the control embryos ($p < 0.05$). One pluripotency repressor gene, *GADD45G*, was lower in the *XIST*-deficient embryos than in the control embryos. *POU5F1*, which is expressed in both ICM and trophectoderm in pig, showed higher expression level in control embryos (Figure 3D).

Histone modification also plays an important role in reprogramming, and H3K9me3 was proved to be the epigenetic barrier for producing fully reprogrammed pluripotent stem cells (Chen et al., 2013). Hence, the expression level of two H3K9me3 demethylases (*Kdm4A/4B*), and the corresponding methyltransferases *SUV39h1* and *SETDB1*, were particularly defined by qRT-PCR. We found only *Kdm4A* but not *Kdm4B* exhibited a prominently higher expression level in the *XIST*-null embryos than in the control embryos. By contrast, *SUV39h1* only expressed in the control embryos and somatic donor cells, but not in the IVF embryos and the *XIST*-null embryos. *Kdm4B* exhibited very low expression levels in all three group embryos and showed no significant difference in the control, *XIST*-null, and IVF embryos (Figure 3E). We confirmed our results by further examining the global H3K9me3 level through immunostaining of the IVF, PA, control, and *XIST*-null embryos (Figure 3F). The global H3K9me3 level in *XIST*-null embryos decreased significantly compared with those in the control and PA embryos, but was close to that in the fertilized embryos.

Effects of H3K9me3 Demethylase Addition on Development Capacity and Gene Expression Pattern of NT Embryos

We retrospectively analyzed the dynamic change of expression pattern of *Kdm4A*, *Kdm4B*, *SUV39h1*, and *SETDB1* in the early stage of IVF embryos based on published RNA-seq data (Cao et al., 2014). For the two demethylases, *Kdm4A* expression was not detectable in one- and two-cell-stage embryos, but dramatically increased from four- to eight-cell stage (ZGA phage), and *Kdm4B* expression remained at a very low level and did not exhibit a large change from one-cell stage to blastocyst stage. For methyltransferases, *SUV39h1* was undetectable during the whole pre-implantation stage, and *SETDB1* showed a high-expression level in one- to two-cell-stage embryos, but became undetectable after the four-cell stage (Figure 4A). Based on these retrospective analysis data we postulated that demethylases might play a vital role in early pre-implantation of embryos. To verify the hypotheses, synthesized mRNAs of three porcine polyadenylated H3K9me3 demethylases, *Kdm4A*, *Kdm4B*, and *Kdm4D* were injected separately into the reconstructed NT embryos derived from wide-type fetal fibroblasts 5 hr after activation (Figure S4A). In the initial comparison experiments, we found that global H3K9me3 level reduced by *Kdm4A* addition was much higher than that of *Kdm4B* and *Kdm4D* injection; *Kdm4A* addition also resulted in a higher blastocyst rate (83/224, 37%, n = 3) than *Kdm4B* (55/237, 23.2%, n = 3), *Kdm4D* (27/150, 18%, n = 3), and the control (31/146, 21.2%, n = 3) (Figures S4B and S4C). To reaffirm the beneficial effect of *Kdm4A* on pig SCNT, we reconstructed 802 additional SCNT embryos with the wild-type donor cells.

Figure 3. Gene Expression Related to Pluripotency and Epigenetics Status in Reconstructed Embryos Derived from *XIST*-Null Donor Cells

(A) Methylation statuses of the *POU5F1*, *XIST*, and *IGF2* loci in the female donor cells and day 6 SCNT embryos. IVF embryos were mixture of female and male embryos. Solid-filled circles represent the methylated cytosine, whereas open circles represent the unmethylated cytosine in each CpG site. The horizontal line represents one individual clone. The left diagram in each figure denotes the genomic location of the target DNA methylation region.

(B) RNA-seq analysis (Spearman correlation coefficient) of the fertilized, *XIST*-KO and wild-type embryos.

(C) GO analysis of genes inactivated in wild-type embryos while activated in *XIST*-KO embryos.

(D) Hierarchical cluster analysis of IVF, XIST-deficient and wild-type cell-derived embryos. Yellow and purple represent higher and lower gene expression levels, respectively.

(E) Relative expression levels of H3K9me3 demethylases (*Kdm4A/B*) and methyltransferases (*SUV39h1* and *SETDB1*) in *XIST*-KO, wild-type and IVF embryos by qRT-PCR (n = 3 biological replicates, Error bars indicate SEM, $*p < 0.05$, $**p < 0.01$, two-tailed unpaired Student's t test).

(F) Immunofluorescent staining of global H3K9me3 in fertilized embryos, parthenogenetic embryos, wild-type embryos, and *XIST*-null embryos. Three independent experiments. Scale bars, 100 μm.

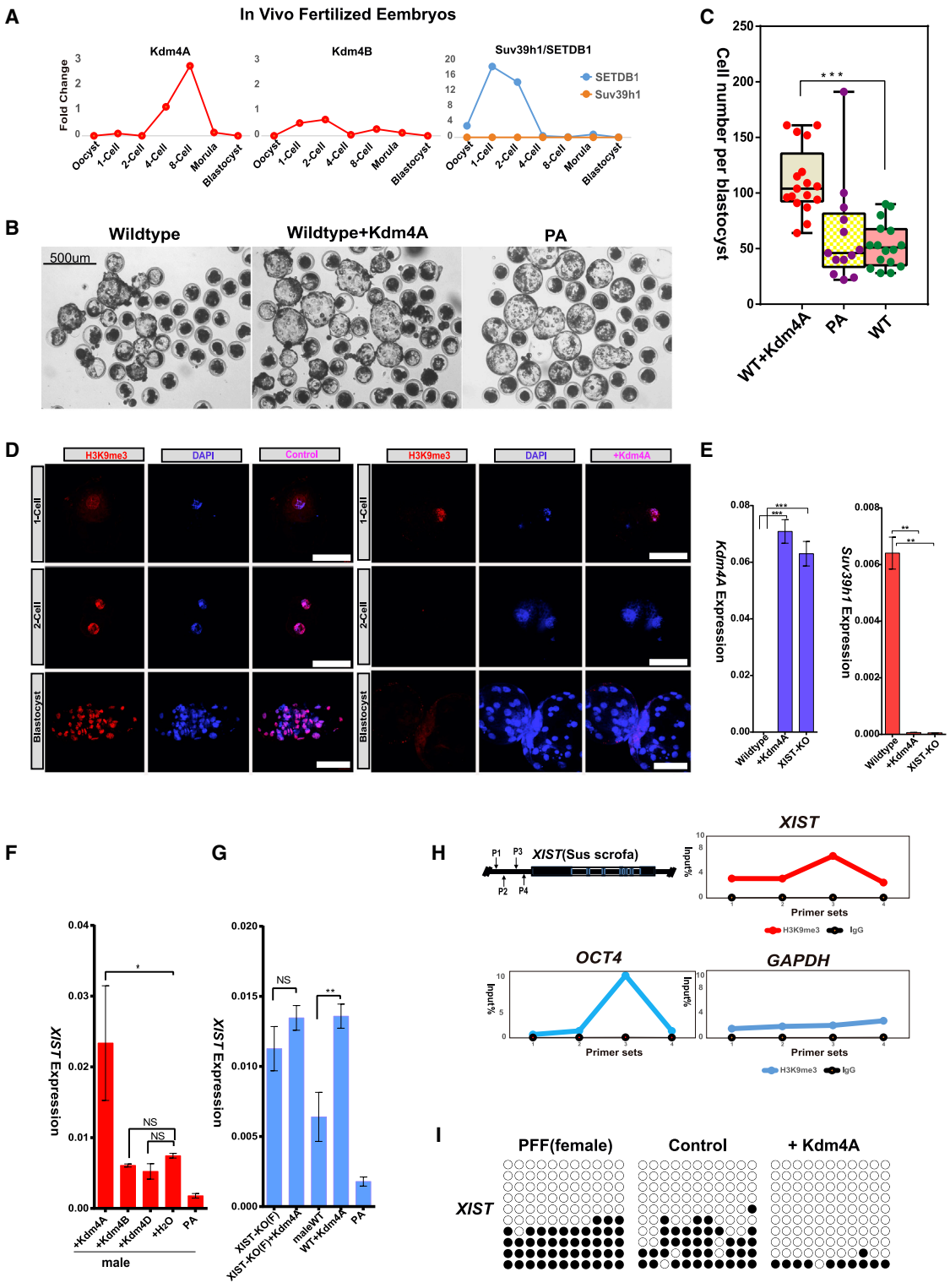

Figure 4. The Influence of Addition of *Kdm4A* on the Quality of NT Embryos

(A) *Kdm4A*, *Kdm4B*, *Suv39h1*, and *SETDB1* expression pattern in the early stage of *in vivo* fertilized embryos.

(B) *Kdm4A* injection greatly increased blastocyst rate and helped *in vitro* culture embryos develop to the hatched stage, Scale bar, 500 μm.

(legend continued on next page)

Kdm4A mRNA was injected into 428 embryos at 5 hr after activation, and the remaining 374 embryos served as non-injected controls (Table S4). We followed the early developmental process of these SCNT embryos, and found that *Kdm4A* addition significantly increased the blastocyst rate (+*Kdm4A* 129/368, 35% versus control 92/367, 25%, n = 6) ($p < 0.01$) (Table S4), although it did not affect the development of the two- and four-cell embryo formation (Figure S4C). Addition of *Kdm4A* also increased in the number of hatched embryos (Figures 4B and S4D) and the cell number per blastocyst after *in vitro* culture with serum on day 6 (+*Kdm4A* 110 versus control 53, $p < 0.001$) in the *Kdm4A*-injection group (Figures 4C and S4E).

We transferred 654 *Kdm4A*-injected embryos and 485 control NT embryos into the same 8 surrogates, 4 of them were pregnant, and 3 piglets coming *Kdm4A*-injected embryos were delivered. The *in vivo* developmental capacity of the NT embryos after injection of H3K9me3 demethylase *Kdm4A* was not enhanced (3/654, 0.46%) (Table S4).

We further examined if addition of *Kdm4A* could influence *Xist* expression. The fertilized, *XIST*-KO and wild-type cell-derived embryos were used as control. First, immunostaining revealed the presence of global H3K9me3 in the one-cell-stage embryos, but not in the two-cell-stage and blastocyst-stage embryos in *Kdm4A*-injected embryos (Figure 4D). Moreover, *Kdm4A* addition greatly increased *Kdm4A* while it reduced *SUV39h1* expression level of day 6 *in vitro* blastocysts (Figure 4E). By contrast, *Kdm4A*, but not *Kdm4B* or *Kdm4D* addition, significantly elevated *Xist* expression level (Figure 4F) in wild-type cell-derived embryos, but not affect that in the embryos derived from the *XIST*-null donor cells (Figure 4G). Chromatin immunoprecipitation (ChIP)-qPCR further revealed that in the donor fibroblasts, *XIST* promoter was enriched with H3K9me3 (Figure 4H). Bisulfite sequence analysis showed that the DNA methylation level substantially decreased by *Kdm4A* addition on the *XIST* loci (+*Kdm4A* 10% versus control 34.5%) (Figure 4I), which would lead to *Xist* upregulation.

We next compared the embryo transcriptome of all groups in genome-wide scale by Spearman correlation analysis and PCA analysis. The results revealed that transcription pattern of *Kdm4A* injection embryos were similar to *XIST*-null embryos rather than to IVF embryos and wild-type cell-derived embryos (Figures S4F and S4G). Linear correlation analysis revealed that the correlation factor between *Kdm4A* addition embryos and IVF embryos was 0.929 (R), very close to that of *XIST*-KO embryos (R = 0.92) (Figure S4H). Genes up- and downregulated in *Kdm4A* addition embryos also distributed across all the chromosomes (Figures S4I and S4J). Compared with *XIST*-KO embryos, the number of specially upregulated genes were decreased in *Kdm4A* addition embryos (*XIST*-KO 608 versus *Kdm4A* 375), while the number of specially downregulated genes in *Kdm4A* addition embryos was increased, even though it was fewer than in the control embryos (*Kdm4A* 628 versus *XIST*-KO 154 versus control 1,091) (Figure S4K). The up- and downregulated genes in *Kdm4A* addition embryos were also distributed across every chromosome (Figure S4L).

DISCUSSION

In the present study, we systematically analyzed the gene expression profile of porcine pre- and post-implantation embryos and found that fertilized, SCNT embryos featured different global transcriptome patterns. The level of change in the normal embryos was smaller than that in the abnormal ones. There were more CUGs in the normal fetuses than those in abnormal fetuses (475 versus 267 in post-implantation fetuses). GO analysis revealed that the genes that failed to be activated in the abnormal fetuses were enriched in embryo development pathways. By contrast, the CUGs in the abnormal fetuses seemed involved in different functions, such as metabolism. The difference in the total number of CDGs between the abnormal and normal fetuses (805 versus 120 in post-implantation fetuses) appeared much more striking than the number of upregulated genes. These CDGs existed not only in the X chromosome, but also in autosomes. In

(C) *Kdm4A* injection (n = 17) significantly increased the total cell number per blastocyst on day 6 (with 10% fetal bovine serum from day 4) in *in vitro* culture (embryos from three independent replicates). Error bars indicate SEM, ***$p < 0.001$, two-tailed unpaired Student's t test.
(D) Immunofluorescent assay showed that *Kdm4A* addition at 5 hr post-activation can significantly reduce the global H3K9me3 levels of NT embryos, Scale bars, 100 μm.
(E) *Kdm4A* addition greatly upregulated *Kdm4A* in day 6 blastocysts, while downregulated *SUV39h1*. Error bars indicate SEM, n = 3 independent replicates, **$p < 0.01$, ***$p < 0.001$, two-tailed unpaired Student's t test.
(F and G) *Kdm4A* injection but not *Kdm4B/D* injection significantly upregulated *XIST* expression. *Kdm4A* injection significantly upregulated *XIST* expression in wild-type derived cell but not *XIST*-null donor cells. Mean with SEM, n = 3 independent replicates from 3 separate embryo extracts, *$p < 0.05$, **$p < 0.01$, two-tailed unpaired Student's t test.
(H) ChIP-qPCR to show H3K9me3 status of *XIST* promoter of male donor fibroblast cells. The upper left diagram in the figure denotes the genomic location of the primer sets. *OCT4* and *GAPDH* were used as positive and negative control, respectively.
(I) Methylation statuses of the *XIST* loci in the female donor cells and day 6 control and *Kdm4A* addition SCNT embryos.

particular, *Xist*, a long non-coding RNA gene, showed highly ectopic expression (among the top ten) in abnormal fetuses. Consistently, the PRC2 gene expression profile of retarded embryonic day 35 (E35) and E30 fetuses was similar to each other rather than to normal cloned fetuses and fertilized fetuses on E30 and E35.

Previous studies reported that the ectopic Xist expression specially caused chromosome-wide gene downregulation on the X chromosome in mouse cloned embryos (Matoba et al., 2011). However, in pigs, the overall decrease in the expression of the genes in cloned embryos not only happened on the X chromosome but also on the other autosomes. In the mouse, the ectopic Xist expression in cloned embryos was corrected autonomously after implantation in both embryonic and extraembryonic regions. However, in pig, highly anomalous *Xist* expression persisted to post-implantation stage in abnormal fetuses. This may be due to a species difference of *Xist* imprinting pattern. In the mouse, Xist is imprinted at the pre-implantation stages of development, and later is randomly monoallelically expressed, while, in rabbits and humans, imprinting of Xist was not observed, even at pre-implantation stages (Okamoto et al., 2011). For pigs, a *Xist* imprinting pattern has as yet not been established but is probably similar to that of rabbits and humans, since an overall decrease in the expression of the genes was found on both the X chromosome and autosomes.

Compared with the IVF-derived embryos, as in the mouse, SCNT embryos exhibited significantly higher *XIST* transcription levels at the morula stage. The *XIST* gene is not expressed in the Xa of somatic cells because the *XIST* gene promoter is enriched with H3K9me3. When the somatic donor cells are injected into oocytes, H3K9me3 loss for chromatin decondensation is a necessary condition for reprogramming differentiated cells into pluripotent ones, inevitably causing derepression of *XIST*. Therefore, reduction of *XIST* expression will help the development of cloned embryos. In mouse, both the deletion of *XIST* in the donor cells (Inoue et al., 2010) (Marahrens et al., 1997) and the anti-*XIST* siRNA injection at the one-cell-stage embryos (Matoba et al., 2011) could effectively inhibit abnormal *XIST* expression at the morula stage and markedly increase the mouse cloning efficiency. In the pig SCNT embryos, however, a previous report showed that siRNA-mediated *XIST* repression only slightly improved the survival rate of cloned pig embryos (Zeng et al., 2016). The silencing effect of anti-*XIST* siRNA injected at the one-cell stage needed to be maintained for at least 3 days in mouse and 5 days in pig. These durations correspond to the time required for developing from the one-cell stage to the morula stage for the two species. Injected siRNA may degrade before morula formation in the pig (Amarzguioui et al., 2003; Holen et al., 2002; Tuschl, 2002). In the same study, the authors employed several measures to promote the silencing effect of injected anti-*XIST* siRNA. These measures included increasing the concentration of injected anti-*XIST* siRNA by 10-fold; using chemically modified anti-*XIST* siRNA and short hairpin RNA, which were expected to provide a more persistent and stable gene silencing effect than siRNA (Gu et al., 2011); and postponing the injection of anti-*XIST* agents from the one-cell to the two- or four-cell stage. However, all these methods could still not effectively suppress *XIST* expression at the morula stage in the cloned pig embryos (Zeng et al., 2016). In addition, Oikawa et al. (2013) found that the RNAi-mediated knockdown of *XIST* in mouse SCNT embryos does not rescue the impaired development of female cloned mouse embryos (Oikawa et al., 2013). Notably, our qRT-PCR results showed that the abnormal upregulation of *XIST* in the pig existed, not only in the early stage of the pre-implantation embryos but also in the post-implantation stage. This finding is consistent with previous results on *XIST* expression in abnormal fetuses from post-implantation and post-natal-stage embryos (Jiang et al., 2008; Yuan et al., 2014). Thus, contrary to the effect in mouse, the RNAi treatment of oocytes is not applicable for improving SCNT embryo development in pigs.

In the present study, we choose to disrupt the *XIST* gene function of porcine donor cells by inserting an EGFP CDS and a puromycin-resistance cassette downstream of the *XIST* promoter. Consequently, the *XIST* deficiency of donor cells could enhance blastocyst rate and significantly increase average cell number per blastocyst. We also confirmed that the reconstructed embryos from the *XIST*-nullified cells exhibited a higher *in vivo* long-term developmental competency than the embryos derived from the wild-type cells. This conclusion is convincing because we attained four piglets plus seven normal fetuses out of 530 *XIST*-deficient embryos (2.07%) when an equal number of embryos, derived from male *XIST*-deficient cells and wild-type cells, were transferred into the same surrogates. By contrast, we only achieved two piglets plus one normal fetus out of as many as 953 wild-type cell-derived embryos (0.3%). The cloning efficiency under the use of *XIST*-deficient cells as donor nuclei was 6.9 times higher than that under the use of wild-type cells. This result is consistent with the finding of similar works on mice (Inoue et al., 2010; Matoba et al., 2011). The *XIST*-null and normal wild-type fetuses shared highly similar transcriptomes, including the total numbers of up- and downregulated genes and the expression levels of both paternally expressed (*DLK1* and *IGF2*) and maternally expressed (*H19*) genes. Hence, the normal gene expression of cloned embryos normalized by *XIST* nullification in the donor cells could persist to the post-implantation stage and result in enhanced cloning efficiency.

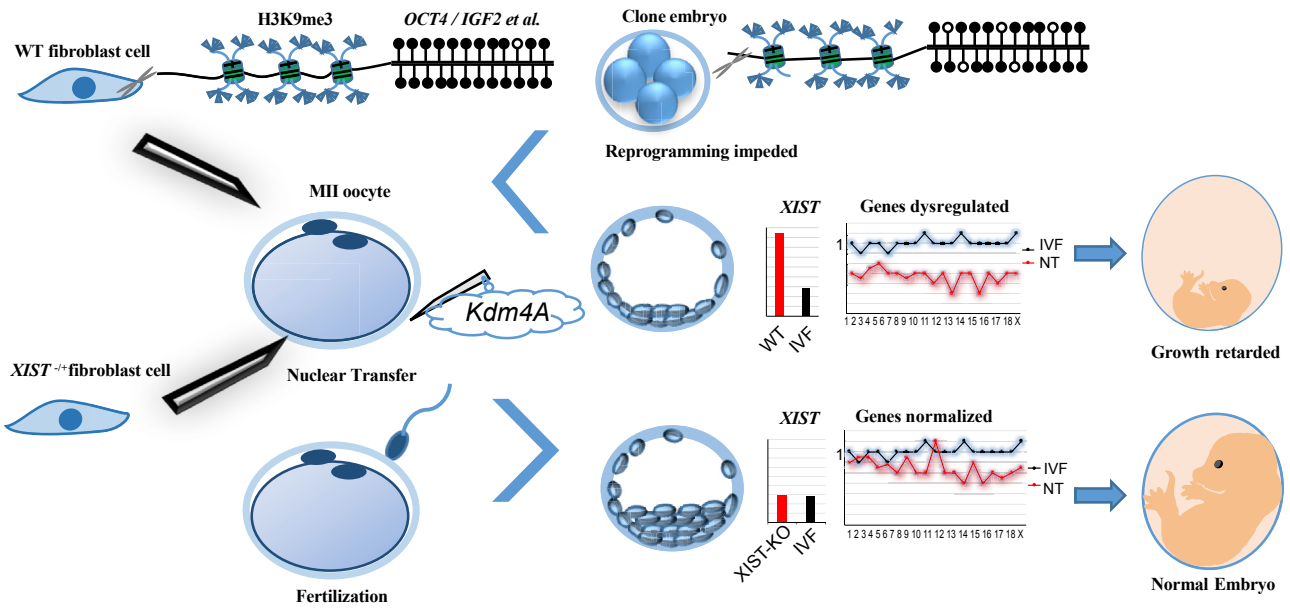

Figure 5. A Model Demonstrating the Influence of *XIST* on Pig SCNT Embryo Development

Many SCNT embryos undergo growth retardation in the post-implantation stage because of incomplete reprogramming. H3K9me3 and DNA methylation are the barriers impeding the reprogramming process. In the early pre-implantation stage of the NT embryo development, H3K9me3 loss for chromatin decondensation seems inevitable. Global H3K9me3 level decreases (as *Kdm4A* injection) and DNA demethylation in *XIST* promoter during reprogramming, which causes *XIST* elevation and thus hinders embryo developmental capacity of the NT embryos. Through *XIST* gene nullification, the global H3K9me3 level and the DNA methylation level in specific locus are substantially reduced and result in enhanced embryo competency to develop full term.

The mechanism of the beneficial influence of *XIST* deficiency on the development of early-stage cloned embryos is poorly understood. Our results showed that the nullification of the *XIST* gene of donor cells for SCNT could normalize the aberrant expression of many genes in the early stage of cloned embryos. The expression levels of pluripotency-regulating genes, such as *GATA4* and *ZFP42*, were elevated, whereas those of pluripotency repressor genes were downregulated in the *XIST*-deficient embryos. DNA demethylation levels of some transcription factors and imprinted genes, including *POU5F1*, *XIST,* and *IGF2,* which can reflect reprogramming completion degree, were decreased in the embryos derived from *XIST*-deficient cells and became more identical to those in IVF embryos. The expression levels of genes related to histone modification in cloned embryos, which are considered to play important roles in embryo development (Diao et al., 2014; Gao et al., 2010; Park et al., 2011; Zhou et al., 2014) and in reprogramming differentiated cells into pluripotent stem cells (Chen et al., 2013; Rais et al., 2013), became similar to those of the fertilized embryos. The H3K9me3 level, which was considered as a main epigenetic barrier of reprogramming (Chen et al., 2013), became lower and more identical to the level of the IVF embryos in the *XIST*-null embryos than in the control embryos. Among all the H3K9me3 regulators, H3K9me3 demethylase *Kdm4A* showed most prominently high-expression levels in the *XIST*-null embryos. More notably, H3K9me3 methyltransferase *Suv39h1*, which was expressed in somatic cells and wild-type cell-derived cloned embryos, but not in IVF embryos, became undetectable in *XIST*-null embryos. All the above molecular changes are favorable for the development of cloned embryos.

A previous study on mice demonstrated that the inactivation of histone demethylases accounts for the arrest of cloned embryo development, and the addition of histone demethylases Kdm4b and Kdm5b in one-cell-stage embryos to reduce H3K9me3 and H3K4me3 levels, respectively, could improve both pre- and post-implantation developmental capacity of cloned embryos (Liu et al., 2016). For pigs, we tentatively injected *Kdm4A*, *Kdm4B*, and *Kdm4D* into one-cell-stage cloned embryos and found that *Kdm4A* was able to improve development of pre-implantation stage embryos. However, the *in vivo* long-term developmental capacity of the NT embryos after injection of H3K9me3 demethylase *Kdm4A* was not enhanced. The addition of *Kdm4A* could result in some positive changes prone to cloned embryo development at the molecular level, such as no H3K9me3 methyltransferase *SUV39h1* expression or reduction of global H3K9me3 levels.

However, addition of *Kdm4A* significantly elevated *XIST* expression, thus hindering the developmental capacity of pig NT embryos.

In summary, our results demonstrated that nullification of the *XIST* gene in donor cells can normalize aberrant gene expression in cloned embryos and enhance long-term development capacity of embryos, which were mediated by downregulation of H3K9me3 levels (Figure 5). Injection of *Kdm4A* into NT embryos, on the one hand, can improve oocyte reprogramming with increased blastocyst rate and total cell number per blastocyst. However, addition of *Kdm4A* significantly elevated *XIST* expression, which would hinder the developmental capacity of pig NT embryos. Therefore, injecting *Kdm4A* mRNA into reconstructed SCNT embryos, such as that in mouse, may not applicable for generating genome-modified pig models.

EXPERIMENTAL PROCEDURES

All experimental protocols involving the use of pigs were approved by the Institutional Animal Care and Use Committee at Guangzhou Institute of Biomedicine and Health, Chinese Academy of Sciences (Animal Welfare Assurance no. A5748-01).

RNA-Seq Data Process

Illumina bcl2fastq (v.1.8.4) was used for base calling. Reads were trimmed for adaptor sequence, and masked for low-complexity or low-quality. Then, the clean reads were mapped to pig genome by RSEM (rsem-1.2.4) (Li and Dewey, 2011), genome files used SGSC Sscrofa10.2/susScr3, gene referenced file came from NCBI. Transcripts per million normalized counts were used for the downstream analysis. PCA, hierarchical cluster, etc., were performed by local Python scripts based on scikit-learn, Matplotlib, Seaborn, etc.

Chromatin Immunoprecipitation-qPCR

The procedure of ChIP was carried out as described previously (Chen et al., 2013). Basically, pig fetal fibroblasts suspended in fibroblast culture medium were crosslinked with 1% formaldehyde for 10 min at room temperature. Then, using 125 mM glycine to quench formaldehyde; subsequently, cells were washed twice with cold PBS. Cells were then lysed in ChIP buffer A for 10 min at 4°C. Samples were centrifuged at 1,400 × *g* for 5 min at 4°C. Pellets were resuspended in ChIP buffer B for 10 min at 4°C and were sheared by sonication. Sheared chromatin was centrifuged to discard the pellets, and the supernatant was diluted with ChIP IP buffer. Chromatin was incubated with protein A or G beads conjugated to anti-H3K9me3 antibodies (Abcam, ab8898) or rabbit IgG (Abcam, ab37415) overnight at 4°C in ChIP buffer. After immunoprecipitation, beads were washed with low-salt wash buffer, high-salt wash buffer, LiCl wash buffer, and Tris-EDTA buffer. DNA was extracted and used for analysis. The sequences of all primers used in this study are given in the Supplemental Information (Table S2).

Statistical Analyses

Values are reported as the means ±SEM. The p values were calculated by Student's t test, $p < 0.05$ was considered statistically significant. All graphs were plotted with GraphPad Prism software.

ACCESSION NUMBERS

Data from this study are available in GSE107302.

SUPPLEMENTAL INFORMATION

Supplemental Information includes Supplemental Experimental Procedures, four figures, and five tables and can be found with this article online at https://doi.org/10.1016/j.stemcr.2017.12.015.

AUTHOR CONTRIBUTIONS

D.R., K.W., X.L., and L.L. designed the study. D.R., J.P., Y.Y., J.Z., F.C., W.G., H.W., Z.Z., Q.L., Q.J., H.S., J.X., H.S., X.Y.Y., and X.Y. performed the experiments. D.R. and X.W. analyzed the data. Z.O., B.Z., Q.Z., C.L., N.F., and N.L. performed SCNT. Z.L. and Y.Z. performed the embryos transfer experiments. D.R., K.W., and L.L. prepared the manuscript. All authors read and approved the final manuscript.

ACKNOWLEDGMENTS

This work was supported by the National Natural Science Foundation of China (grant nos. 31601187, 31401271, 81671121, and 81672317), the Science and Technology Planning Project of Guangdong Province, China (grant nos. 2014B020225003, 2015A030310119, 2016A020216023, and 2016A030303046), the Youth Innovation Promotion Association CAS (grant nos. 2017409 and 2016317), the Pearl River Nova Program of Guangzhou (201710010112), the Bureau of International Cooperation, the Chinese Academy of Sciences (154144KYSB20150033), the Bureau of Science and Technology of Guangzhou Municipality (201505011111498), and the Science and Technology Planning Project of Guangdong Province, China (grant no. 2017B030314056)

Received: April 13, 2017
Revised: December 16, 2017
Accepted: December 18, 2017
Published: January 11, 2018

REFERENCES

Amarzguioui, M., Holen, T., Babaie, E., and Prydz, H. (2003). Tolerance for mutations and chemical modifications in a siRNA. Nucleic Acids Res. *31*, 589–595.

Bao, S., Miyoshi, N., Okamoto, I., Jenuwein, T., Heard, E., and Azim Surani, M. (2005). Initiation of epigenetic reprogramming of the X chromosome in somatic nuclei transplanted to a mouse oocyte. EMBO Rep. *6*, 748–754.

Brockdorff, N. (2017). Polycomb complexes in X chromosome inactivation. Philos. Trans. R. Soc. Lond. B Biol. Sci. *372*.

Cao, S., Han, J., Wu, J., Li, Q., Liu, S., Zhang, W., Pei, Y., Ruan, X., Liu, Z., Wang, X., et al. (2014). Specific gene-regulation networks

during the pre-implantation development of the pig embryo as revealed by deep sequencing. BMC Genomics *15*, 4.

Cerase, A., Pintacuda, G., Tattermusch, A., and Avner, P. (2015). Xist localization and function: new insights from multiple levels. Genome Biol. *16*, 166.

Chen, J., Liu, H., Liu, J., Qi, J., Wei, B., Yang, J., Liang, H., Chen, Y., Chen, J., Wu, Y., et al. (2013). H3K9 methylation is a barrier during somatic cell reprogramming into iPSCs. Nat. Genet. *45*, 34–42.

Chung, Y.G., Matoba, S., Liu, Y., Eum, J.H., Lu, F., Jiang, W., Lee, J.E., Sepilian, V., Cha, K.Y., Lee, D.R., et al. (2015). Histone demethylase expression enhances human somatic cell nuclear transfer efficiency and promotes derivation of pluripotent stem cells. Cell Stem Cell *17*, 758–766.

da Rocha, S.T., and Heard, E. (2017). Novel players in X inactivation: insights into Xist-mediated gene silencing and chromosome conformation. Nat. Struct. Mol. Biol. *24*, 197–204.

Diao, Y.F., Oqani, R.K., Li, X.X., Lin, T., Kang, J.W., and Jin, D.I. (2014). Changes in histone H3 lysine 36 methylation in porcine oocytes and preimplantation embryos. PLoS One *9*, e100205.

Gao, Y., Hyttel, P., and Hall, V.J. (2010). Regulation of H3K27me3 and H3K4me3 during early porcine embryonic development. Mol. Reprod. Dev. *77*, 540–549.

Gu, S., Jin, L., Zhang, F., Huang, Y., Grimm, D., Rossi, J.J., and Kay, M.A. (2011). Thermodynamic stability of small hairpin RNAs highly influences the loading process of different mammalian Argonautes. Proc. Natl. Acad. Sci. USA *108*, 9208–9213.

Holen, T., Amarzguioui, M., Wiiger, M.T., Babaie, E., and Prydz, H. (2002). Positional effects of short interfering RNAs targeting the human coagulation trigger tissue factor. Nucleic Acids Res. *30*, 1757–1766.

Huan, Y., Zhu, J., Huang, B., Mu, Y., Kong, Q., and Liu, Z. (2015). Trichostatin A rescues the disrupted imprinting induced by somatic cell nuclear transfer in pigs. PLoS One *10*, e0126607.

Huang, Y., Ouyang, H., Yu, H., Lai, L., Pang, D., and Li, Z. (2013). Efficiency of porcine somatic cell nuclear transfer – a retrospective study of factors related to embryo recipient and embryos transferred. Biol. Open *2*, 1223–1228.

Inoue, K., Kohda, T., Sugimoto, M., Sado, T., Ogonuki, N., Matoba, S., Shiura, H., Ikeda, R., Mochida, K., Fujii, T., et al. (2010). Impeding Xist expression from the active X chromosome improves mouse somatic cell nuclear transfer. Science *330*, 496–499.

Jiang, L., Lai, L., Samuel, M., Prather, R.S., Yang, X., and Tian, X.C. (2008). Expression of X-linked genes in deceased neonates and surviving cloned female piglets. Mol. Reprod. Dev. *75*, 265–273.

Lai, L., Kolber-Simonds, D., Park, K.W., Cheong, H.T., Greenstein, J.L., Im, G.S., Samuel, M., Bonk, A., Rieke, A., Day, B.N., et al. (2002). Production of alpha-1,3-galactosyltransferase knockout pigs by nuclear transfer cloning. Science *295*, 1089–1092.

Li, B., and Dewey, C.N. (2011). RSEM: accurate transcript quantification from RNA-seq data with or without a reference genome. BMC Bioinformatics *12*, 323.

Liu, W., Liu, X., Wang, C., Gao, Y., Gao, R., Kou, X., Zhao, Y., Li, J., Wu, Y., Xiu, W., et al. (2016). Identification of key factors conquering developmental arrest of somatic cell cloned embryos by combining embryo biopsy and single-cell sequencing. Cell Discov. *2*, 16010.

Mao, J., Tessanne, K., Whitworth, K.M., Spate, L.D., Walters, E.M., Samuel, M.S., Murphy, C.N., Tracy, L., Zhao, J., and Prather, R.S. (2012). Effects of combined treatment of MG132 and scriptaid on early and term development of porcine somatic cell nuclear transfer embryos. Cell Reprogram. *14*, 385–389.

Mao, J., Zhao, M.T., Whitworth, K.M., Spate, L.D., Walters, E.M., O'Gorman, C., Lee, K., Samuel, M.S., Murphy, C.N., Wells, K., et al. (2015). Oxamflatin treatment enhances cloned porcine embryo development and nuclear reprogramming. Cell Reprogram. *17*, 28–40.

Marahrens, Y., Panning, B., Dausman, J., Strauss, W., and Jaenisch, R. (1997). Xist-deficient mice are defective in dosage compensation but not spermatogenesis. Genes Dev. *11*, 156–166.

Matoba, S., Inoue, K., Kohda, T., Sugimoto, M., Mizutani, E., Ogonuki, N., Nakamura, T., Abe, K., Nakano, T., Ishino, F., et al. (2011). RNAi-mediated knockdown of Xist can rescue the impaired post-implantation development of cloned mouse embryos. Proc. Natl. Acad. Sci. USA *108*, 20621–20626.

Matoba, S., Liu, Y., Lu, F., Iwabuchi, K.A., Shen, L., Inoue, A., and Zhang, Y. (2014). Embryonic development following somatic cell nuclear transfer impeded by persisting histone methylation. Cell *159*, 884–895.

Meissner, A., and Jaenisch, R. (2006). Mammalian nuclear transfer. Dev. Dyn. *235*, 2460–2469.

Ogura, A., Inoue, K., and Wakayama, T. (2013). Recent advancements in cloning by somatic cell nuclear transfer. Philos. Trans. R. Soc. Lond. B Biol. Sci. *368*, 20110329.

Oikawa, M., Matoba, S., Inoue, K., Kamimura, S., Hirose, M., Ogonuki, N., Shiura, H., Sugimoto, M., Abe, K., Ishino, F., et al. (2013). RNAi-mediated knockdown of Xist does not rescue the impaired development of female cloned mouse embryos. J. Reprod. Dev. *59*, 231–237.

Okamoto, I., Patrat, C., Thepot, D., Peynot, N., Fauque, P., Daniel, N., Diabangouaya, P., Wolf, J.P., Renard, J.P., Duranthon, V., et al. (2011). Eutherian mammals use diverse strategies to initiate X-chromosome inactivation during development. Nature *472*, 370–374.

Park, K.E., Johnson, C.M., Wang, X., and Cabot, R.A. (2011). Differential developmental requirements for individual histone H3K9 methyltransferases in cleavage-stage porcine embryos. Reprod. Fertil. Dev. *23*, 551–560.

Park, K.W., Cheong, H.T., Lai, L., Im, G.S., Kuhholzer, B., Bonk, A., Samuel, M., Rieke, A., Day, B.N., Murphy, C.N., et al. (2001). Production of nuclear transfer-derived swine that express the enhanced green fluorescent protein. Anim. Biotechnol. *12*, 173–181.

Rais, Y., Zviran, A., Geula, S., Gafni, O., Chomsky, E., Viukov, S., Mansour, A.A., Caspi, I., Krupalnik, V., Zerbib, M., et al. (2013). Deterministic direct reprogramming of somatic cells to pluripotency. Nature *502*, 65–70.

Rodriguez-Osorio, N., Urrego, R., Cibelli, J.B., Eilertsen, K., and Memili, E. (2012). Reprogramming mammalian somatic cells. Theriogenology *78*, 1869–1886.

Schultz, R.M. (2002). The molecular foundations of the maternal to zygotic transition in the preimplantation embryo. Hum. Reprod. Update *8*, 323–331.

Tuschl, T. (2002). Expanding small RNA interference. Nat. Biotechnol. *20*, 446–448.

Yuan, L., Wang, A., Yao, C., Huang, Y., Duan, F., Lv, Q., Wang, D., Ouyang, H., Li, Z., and Lai, L. (2014). Aberrant expression of Xist in aborted porcine fetuses derived from somatic cell nuclear transfer embryos. Int. J. Mol. Sci. *15*, 21631–21643.

Zeng, F., Huang, Z., Yuan, Y., Shi, J., Cai, G., Liu, D., Wu, Z., and Li, Z. (2016). Effects of RNAi-mediated knockdown of Xist on the developmental efficiency of cloned male porcine embryos. J. Reprod. Dev. *62*, 591–597.

Zhao, M.T., Rivera, R.M., and Prather, R.S. (2013). Locus-specific DNA methylation reprogramming during early porcine embryogenesis. Biol. Reprod. *88*, 48.

Zhou, N., Cao, Z., Wu, R., Liu, X., Tao, J., Chen, Z., Song, D., Han, F., Li, Y., Fang, F., et al. (2014). Dynamic changes of histone H3 lysine 27 acetylation in pre-implantational pig embryos derived from somatic cell nuclear transfer. Anim. Reprod. Sci. *148*, 153–163.